Supporting Information

MacLellan et al. 10.1073/pnas.0910006106

SI Materials and Methods

Genetic Techniques. Standard DNA manipulation techniques were used throughout this study. Site-directed mutagenesis was carried out using mutagenic complimentary primers and a strategy based on the Stratagene Quikchange mutagenesis method.

In Vivo Expression and Protein Pull-Down Assays. Relevant strains were grown overnight, and this growth was used to inoculate fresh 100-mL volumes of LB broth to OD_{600} of 0.05. After incubation at 37 °C with shaking to OD_{600} of 0.4, cultures were induced with 2% (vol/vol) xylose for 1 h. Induction results in the coexpression of YvrI (carrying a 9-aa FLAG epitope) and YvrHa (carrying a 10-aa hemagglutinin epitope) from separate ectopic locations on the chromosome. After induction, cells were collected and disrupted by sonication and sonicate was treated with 5 units of DNaseI for 30 min at room temperature (RT). After centrifugation, clarified crude lysate was supplemented with 0.5 mL of Ni NTA beads and incubated at 4 °C with slow rotation for 1 h. Beads were washed with phosphate buffer (pH 7.6) containing 300 mM NaCl and placed in disposable columns. Bound His-tagged RNAP and cobinding proteins were eluted with a step gradient consisting of 0.5-mL volumes of the above phosphate buffer containing 40, 80, and 160 mM imidazole. Crude lysate and eluate samples were separated on 12% (vol/vol) SDS/PAGE gels, and proteins were visualized by Coomassie staining or were transferred to PVDF membrane and visualized using anti-FLAG and antihemagglutinin antibodies and secondary antibodies conjugated to alkaline phosphatase.

Protein Purification. *B. subtilis* RNAP, SigA, renatured YvrI (tagged with a FLAG epitope), and YvrHa (tagged with a hemagglutinin epitope) were purified as previously described (1). For some assays, YvrI and YvrHa variants carrying hexahistidine tags were purified as above with the inclusion of a Ni metal affinity chromatography step. SigM was renatured from inclusion bodies and purified as previously described (2). The amino and carboxyl halves of YvrI were also individually expressed as FLAG epitope-tagged derivatives in BL21 (DE3). The amino-terminal polypeptide was insoluble and renatured as for full-length YvrI, whereas the carboxyl terminus was soluble. Both proteins were subsequently purified as described for YvrI.

Electrophoretic Mobility Assays. Each 10-μL binding reaction included <100 pmol end-labeled target DNA carrying either the *oxdC* promoter (150 nt) or a control promoter (the SigA-dependent *yoeB*) on a 110-nt fragment, constant amounts of YvrI and YvrHa, and increasing concentrations of RNAP (see legend for Fig. 2) in 10 mM Tris-HCl (pH 7.8), 20 mM KCl, 10 mM $MgCl_2$, 0.1 mM DTT, and 5% (vol/vol) glycerol. Proteins were preincubated in binding buffer for 15 min at RT before loading a mixture of target and control DNA into each tube. After 15 min of further RT incubation, samples were loaded onto a 6% (vol/vol) nondenaturing polyacrylamide gel running at 100 V. After electrophoresis for 45 min, gel were dried and exposed to a phosphor screen.

In Vitro Pull-Down Assays. For in vitro interaction assays, 50 μg of YvrHa or a control protein (hen egg-white lysozyme) was dialyzed into 20 mM phosphate buffer (pH 7.5) containing 500 mM NaCl and conjugated to NHS-activated beads (GE Lifesciences) in accordance with instructions provided by the manufacturer. After extensive washing in 100 mM Tris-HCl (pH 8.0), conjugated beads were stored in this same buffer as a 50% (vol/vol) bead slurry at 4 °C. A typical experiment involved resuspending 50 μL of the bead slurry in binding buffer [10 mM Tris-HCl (pH 7.8), 200 mM NaCl, 5% (vol/vol) glycerol, 0.5 mM DTT, and 0.5% (vol/vol) triton X-100] and supplementing the suspension with 1 μM test protein. After incubation on ice for 30 min with frequent mixing, the volume was brought to 0.5 mL with binding buffer, beads were allowed to sediment by gravity for 2 min, and the supernatant was removed by aspiration. This wash procedure was repeated three times. Note that because of the density of the beads, centrifugation to sediment beads was not necessary, thus reducing carryover of suspended protein precipitates. After the final wash, the beads were resuspended in 40 μL of SDS/PAGE sample buffer, beads were sedimented, and 30 μL of sample buffer containing dissolved proteins was analyzed by SDS/PAGE using a 14% (vol/vol) polyacrylamide gel. For each experiment, conjugated lysozyme beads were used to control for incidental protein carryover and nonspecific binding of test proteins to conjugated protein, the sepharose bead matrix, or the reaction tube wall.

In Vivo Two-Hybrid Assay. The BACTH system used in this work (3) has been employed extensively to map protein–protein interactions between core RNAP subunits, σ-factor domains, and negatively or positively acting regulatory proteins that function through σ- or RNAP interactions (4–9).

The *E. coli* reporter strain FW Kan O_L2–62 lac (10) was cotransformed with relevant recombinant bait and prey plasmids. Single colonies from each strain were used to inoculate a series of 2-mL volumes of LB broth containing ampicillin (100 μg/mL); kanamycin (50 μg/mL); chloramphenicol (25 μg/mL); and either 0, 1, 2, 4, or 8 μM IPTG. After overnight growth at 37 °C, these cultures were used to inoculate fresh 5-mL volumes of the same broth series to OD_{600} of 0.05. When cultures reached OD_{600} of 0.3 to 0.5, 1-mL volumes were extracted, cells were collected by centrifugation, and pellets were frozen overnight. β-Galactosidase assays were conducted as previously described (11). Each strain was tested in duplicate, and each experiment was conducted at least two times.

In developing this assay for use in our laboratory, we extensively tested various negative control combinations and, in the experiments shown, include data only from the bait or prey plasmid equivalent lacking a fusion insert (i.e., plasmids carrying only the λcI or α-gene sequence). These negative controls usually gave maximal activity values of 20–30 Miller units. For a positive control, each experiment included the pACλcI–β831–1,057 and pBRα-σ^{70}–D581G fusion pairs previously shown to interact with high affinity (7, 8). Data from these assays are not included in figures for clarity purposes but generally gave maximal activity values of ≈800 Miller units. For most of the interactions we tested, the best results were obtained with IPTG concentrations between 0 and 8 μM. Higher concentrations of IPTG often proved inhibitory to cell growth and/or did not contribute to differentiating between positive and negative interactions. Many of the gene fragments were tested in both plasmid backgrounds with similar patterns of reporter gene expression. Some interacting pairs gave very high background readings even when uninduced, and we picked those bait/prey plasmid combinations that gave relatively low background activity for further analysis.

The totality of our interaction data demonstrate the functionality and specificity of polypeptides used for both the two-hybrid

analyses and the in vitro pull-down assays. For example, YvrHa interacts with the amino termini of the β′-subunit and YvrI but not with the β-flap domain or region 4 of YvrI. The amino terminus of YvrI interacts with YvrHa but not with the amino terminus of β′ or the β-flap domain, and YvrI region 4 interacts with the β-flap domain but not with β′ or YvrHa. In every instance in which either the N- or C-terminus of YvrI interacts with a partner, the full-length YvrI fusion also interacts (although usually with a lower apparent affinity). Taken together, the full spectrum of the results indicates that the two-hybrid fusion proteins used herein are indeed expressed and fold into domains functional for interaction.

DNA Footprinting. Potassium permanganate footprinting (12) was conducted using supercoiled plasmid (pSM106) DNA in a 20-μL reaction. Each reaction contained 285 nM *B. subtilis* RNAP and equimolar concentrations of YvrI and YvrHa unless otherwise indicated. Proteins were premixed and stored on ice for 15 min before addition to reaction volume containing a final concentration of 10 mM Tris-HCl (pH 7.8), 10 mM $MgCl_2$, 0.5 mM EDTA, 0.5 mM DTT, and 7.5 mM KCl. Plasmid DNA (1 μg) was added, and samples were incubated at 37 °C for 15 min. Reactions were started by the addition of 1 μL of 40 mM $KMnO_4$ and were stopped after 3 min by the addition of 1 μL of β-mercaptoethanol. Oxidized nucleotides were detected using primer extension, as previously described (1). End-labeled primers 5′-GAAAGAGAAGGTGAAAGGCC and 5′-GACAGAACTGAAAGATCATGC were used to map the nontemplate strand and template strand nucleotides, respectively.

Computational Techniques. BLAST and PSI-BLAST were used to identify elements of similarity between YvrHa and other proteins. Alignments were conducted using ClustalW and by manual manipulation. HTH motif prediction was conducted using a program based on the work of Dodd and Egan (13). Photoshop (Adobe) and ImageQuant v5.2 (GE Lifesciences) were used to improve presentation of digital images without altering their information content.

1. MacLellan SR, Wecke T, Helmann JD (2008) A previously unidentified sigma factor and two accessory proteins regulate oxalate decarboxylase expression in Bacillus subtilis. *Mol Microbiol* 69:954–967.
2. Eiamphungporn W, Helmann JD (2008) The Bacillus subtilis sigma(M) regulon and its contribution to cell envelope stress responses. *Mol Microbiol* 67:830–848.
3. Dove SL, Hochschild A (2001) Bacterial two-hybrid analysis of interactions between region 4 of the sigma(70) subunit of RNA polymerase and the transcriptional regulators Rsd from Escherichia coli and AlgQ from Pseudomonas aeruginosa. *J Bacteriol* 183:6413–6421.
4. Deighan P, Diez CM, Leibman M, Hochschild A, Nickels BE (2008) The bacteriophage lambda Q antiterminator protein contacts the beta-flap domain of RNA polymerase. *Proc Natl Acad Sci USA* 105:15305–15310.
5. Gruber TM, Gross CA (2003) Multiple sigma subunits and the partitioning of bacterial transcription space. *Annu Rev Microbiol* 57:441–466.
6. Leibman M, Hochschild A (2007) A sigma-core interaction of the RNA polymerase holoenzyme that enhances promoter escape. *EMBO J* 26:1579–1590.
7. Nickels BE, Dove SL, Murakami KS, Darst SA, Hochschild A (2002) Protein-protein and protein-DNA interactions of sigma70 region 4 involved in transcription activation by lambdacI. *J Mol Biol* 324:17–34.
8. Nickels BE, et al. (2005) The interaction between sigma70 and the beta-flap of Escherichia coli RNA polymerase inhibits extension of nascent RNA during early elongation. *Proc Natl Acad Sci USA* 102:4488–4493.
9. Yuan AH, Nickels BE, Hochschild A (2009) The bacteriophage T4 AsiA protein contacts the beta-flap domain of RNA polymerase. *Proc Natl Acad Sci USA* 106:6597–6602.
10. Deaconescu AM, et al. (2006) Structural basis for bacterial transcription-coupled DNA repair. *Cell* 124:507–520.
11. Dove SL, Hochschild A (2004) A bacterial two-hybrid system based on transcription activation. *Methods Mol Biol* 261:231–246.
12. Sasse-Dwight S, Gralla JD (1991) Footprinting protein-DNA complexes in vivo. *Methods Enzymol* 208:146–168.
13. Dodd IB, Egan JB (1990) Improved detection of helix-turn-helix DNA-binding motifs in protein sequences. *Nucleic Acids Res* 18:5019–5026.

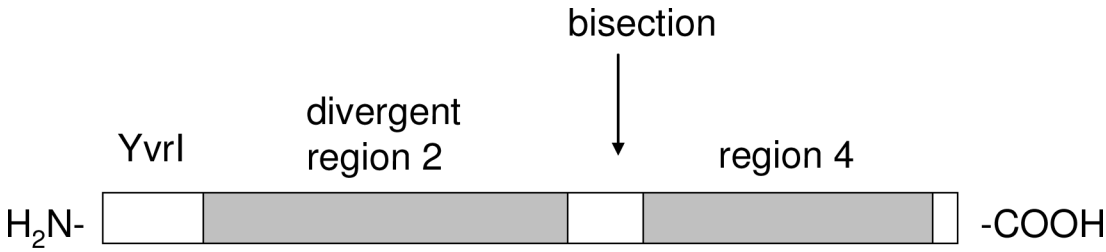

N-terminus (13 kDa)

LMDYQSLLRSKCKEIMKHPIVKHFLSNPQ
HYRLFKNVMESPNEKDARSLDELFKQFY
KEIRIVKYMNSMIRIFSIDFDKRVRKNQKR
YPLTVDHPEAGDRLSSETGSD

C-terminus (10 kDa)

MAFEEFLDRQDDLSQHVQDYQLYQAIQKL
TDKQKSVLTKVYLHGATMQEIADSLGESR
QNI SNIHK KGLENIRKQLAAQKKGEK

Fig. S1. Bisection point of full-length YvrI to generate amino- and carboxy-terminal polypeptides used in two-hybrid analysis and also purified for in vitro interaction assays. Based on multiple sequence alignment with known σ-factors, the approximate dimensions of the divergent regions 2.1–2.4 in the amino terminus and regions 4.1–4.2 in the carboxy terminus are indicated by red text.

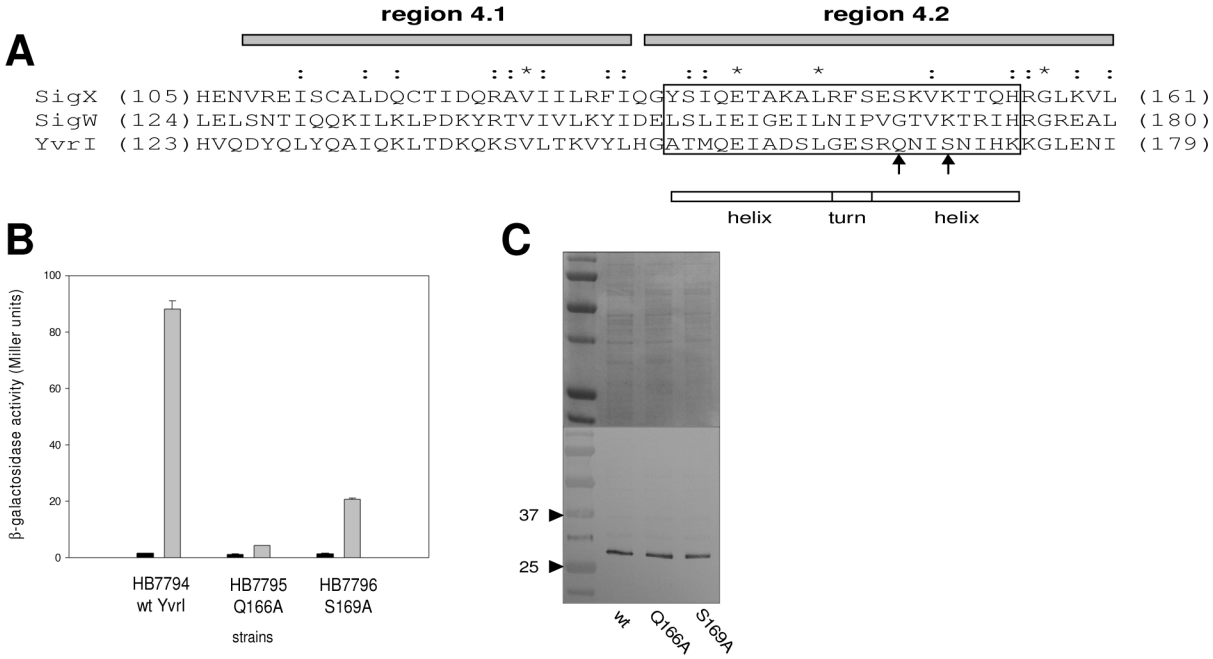

Fig. S2. Effect of mutations in YvrI region 4.2 on transcription in vivo. (*A*) Relevant portion of alignment between two *B. subtilis* ECF σ-factors (SigW and SigX) and YvrI. Coincident HTH motifs are boxed, and residues mutated in YvrI (Q166 and S169) are indicated with vertical arrows. (*B*) Relative in vivo transcription activities from *oxdC* promoter after ectopic induction of WT YvrI and HTH mutant expression (gray bars). Activity from noninduced cells is indicated by black bars. (*C*) Detection of total protein (*Upper*, Coomassie stain) and YvrI (*Lower*, Western immunoblot) expression from strains tested in *B* after induction.

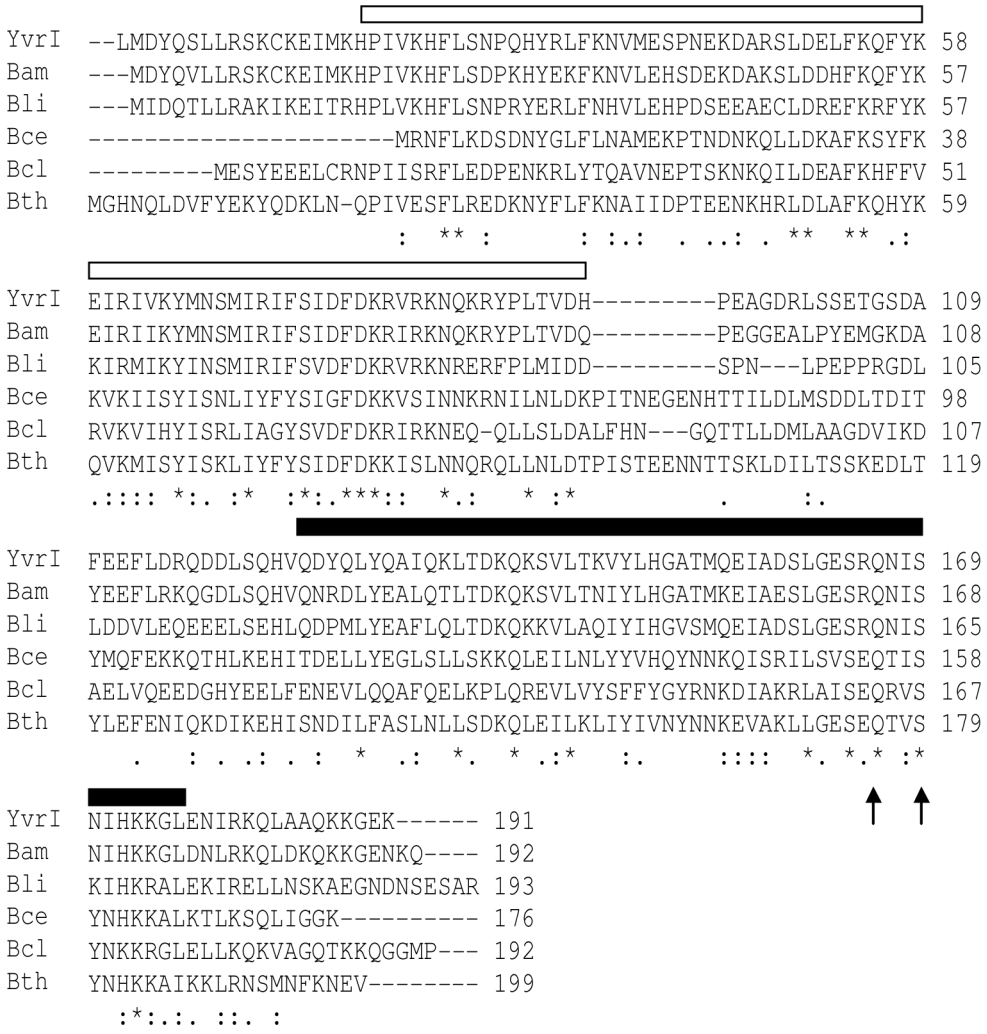

Fig. S3. Alignment of YvrI and homologs from *Bacillus amyloliquefaciens* (Bam), *B. licheniformis* (Bli), *B. cereus* (Bce), *B. clausii* (Bcl), and *B. thuringiensis* (Bth). Conserved residues (Q166 and S169) in the HTH motif mutated for Fig. S2 are indicated with arrows. Approximate dimensions of divergent region 2 and region 4 are indicated by open and closed bars, respectively.

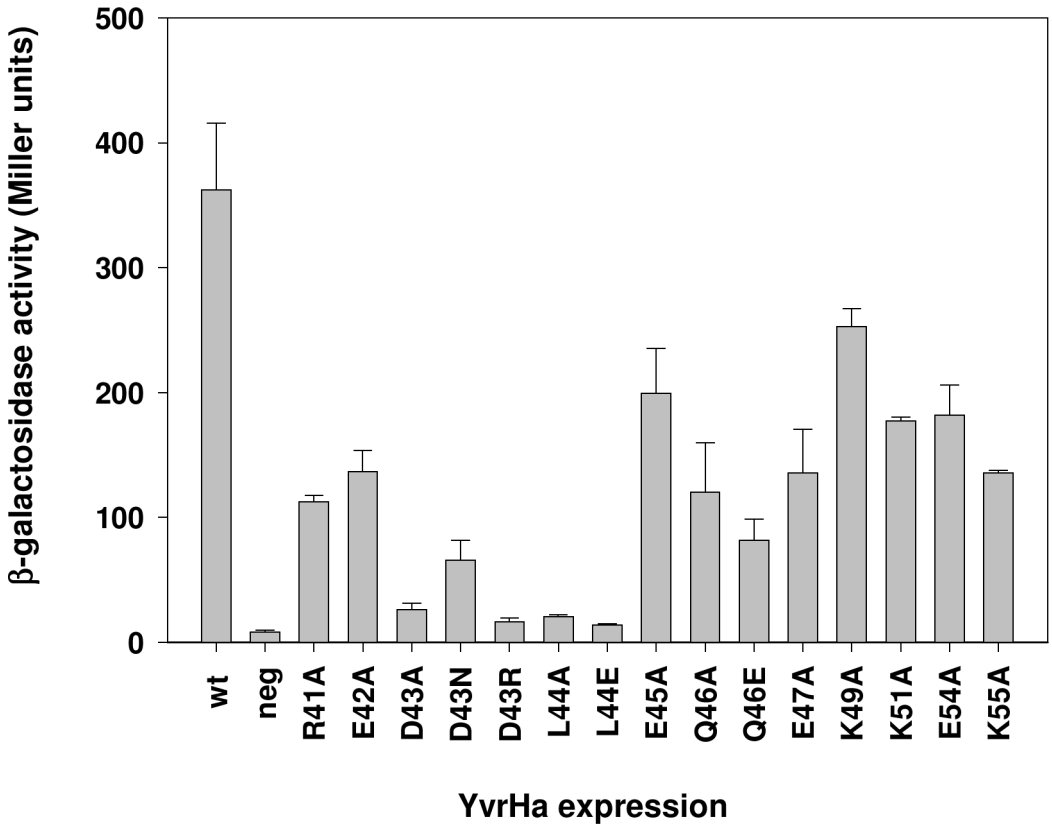

Fig. S4. In vivo transcriptional response to region 2.2 mutations in YvrHa. Conserved YvrHa residues mutated are indicated by asterisks in Fig. 3. YvrI and WT or mutant YvrHa were coexpressed from a xylose-inducible promoter integrated into *amyE* (YvrI) or *lacA* (YvrHa) sites on the chromosome. All mutants are derivatives of pSM019. WT expression is from strain HB7865. The negative control is strain HB7734, which lacks an integrated YvrHa locus. Transcription was monitored from an *oxdC* promoter–*lacZ* fusion integrated into *thrC*. Under these testing conditions, the expression of YvrHa by immunoblotting was not reliable because of low expression. Therefore, the data have not been normalized to control for protein stability.

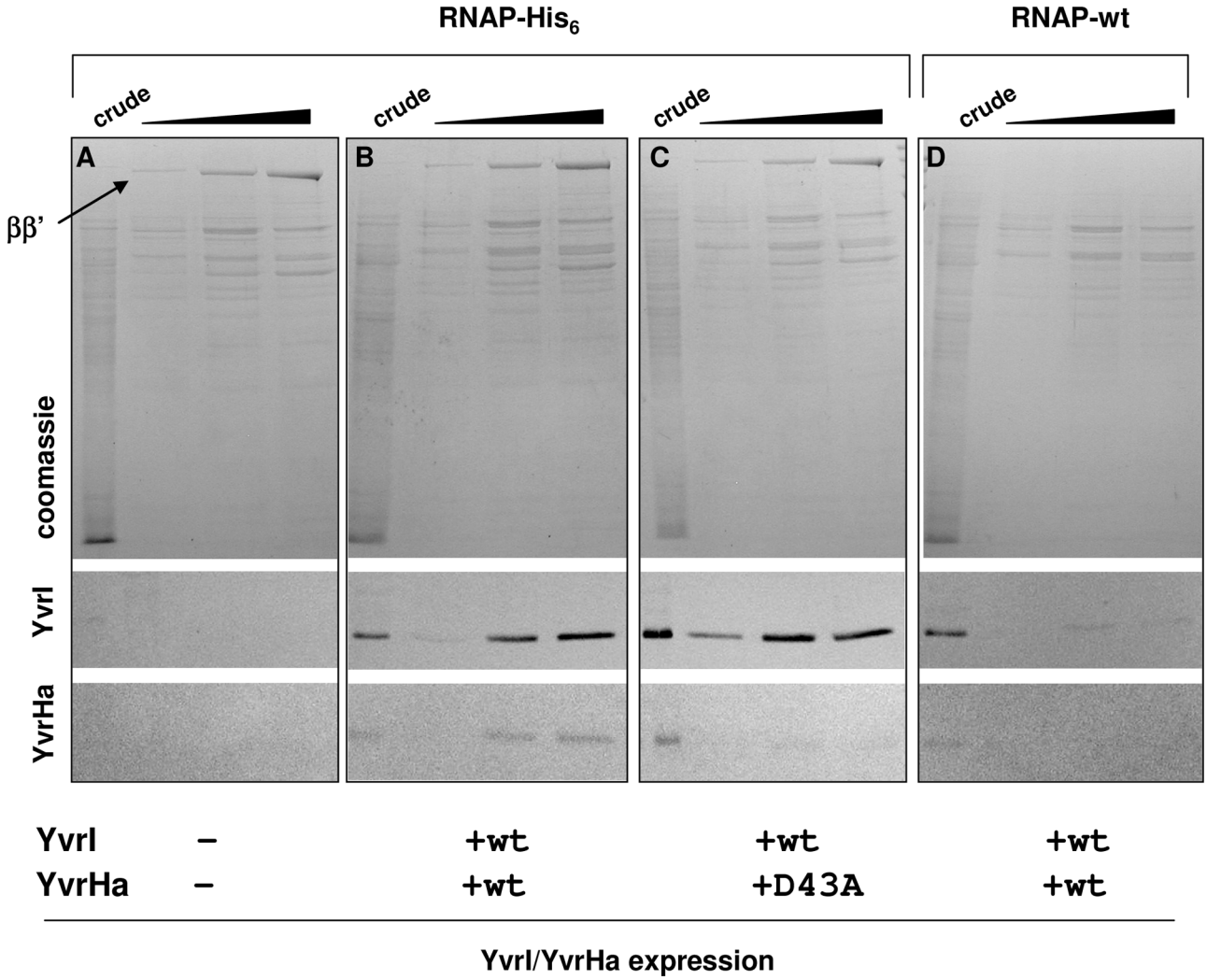

Fig. S5. YvrI and YvrHa expressed in vivo copurify with RNAP. Total protein detection by Coomassie staining (*Upper*) and YvrI (FLAG epitope) and YvrHa (hemagglutinen epitope) immunoblot detection (*Lower*), respectively, from the same samples. In each experiment, cells were disrupted using sonication and crude lysate (labeled crude) was applied to Ni-NTA metal affinity beads to immobilize RNAP carrying a hexahistidine tag (β′-His-6) (see *Materials and Methods*). Captured RNAP-His-6 was eluted from beads with increasing concentrations of imidazole (black triangles) and is visible in Coomassie-stained gels by the presence of ≈150 kDaββ′-bands (*A*, arrow). No induction of YvrI/YvrHa (*A*), induction of WT YvrI/YvrHa (*B*), induction of WT YvrI/D43A YvrHa mutant (*C*), and induction of WT YvrI/YvrHa in genetic background carrying WT (nontagged) RNAP (*D*). This is a composite image generated from a single representative experiment; the original gel and immunoblot images have been compartmentalized for clarity.

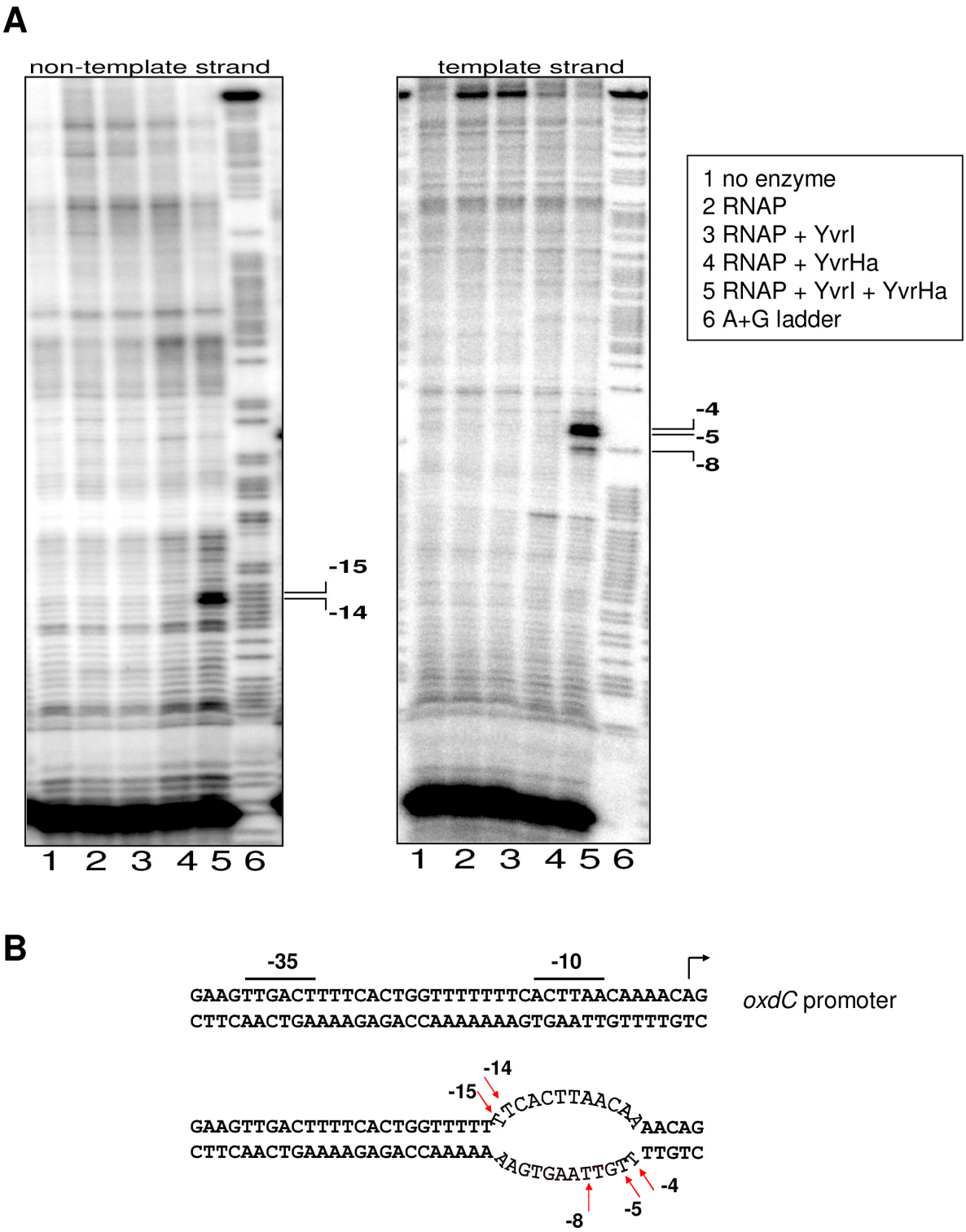

Fig. S6. Open-complex formation at the *oxdC* promoter. (*A*) Complete profile of permanganate reactivity on template and nontemplate strands of a 168-bp fragment, including the *oxdC* promoter region. The identities of hyperoxidized nucleotides were deduced from A+G reactions. (*B*) Nucleotide sequence of the *oxdC* promoter and oxidized bases (red arrows). The dimension of a minimal open-complex region (bubble) was inferred from thymidine reactivity.

Table S1. Strains and plasmids used in this study

Strains	Parental strain, relevant genotype	Source
Escherichia coli		
DH5α	K12 *supE44* Δ*lacU169*(ϕ80*lacZ*ΔM15) *hsdR17 recA1 endA1 gyrA96 thi-1 relA1*	Laboratory collection
BL21 (DE3)	pLysS	Laboratory collection
JM109	*end*A1, *rec*A1, *gyr*A96, *thi, hsd*R17 (r_{k-}, m_k^+), *rel*A1, *sup*E44, Δ(*lac-pro*AB), [F′ *tra*D36, *pro*AB, *laq*I^{q}ZΔM15]	Promega
FW102Kan O_L2–62 lac	FW102 F′ kan pO_L-2–62 lacZ	(1)
Bacillus subtilis		
CU1065	W168 *trpC2 att* SPß	Laboratory collection
MH5636	JH642::*rpoC-His$_{10}$*	M. Hullet
HB7709	CU1065 (pSM002) *amyE*::P$_{xyl}$-*yvrI-FLAG*	This work
HB7711	JH642 PolHis (pSM002) *amyE*::P$_{xyl}$-*yvrI-FLAG*	(2)
HB7720	CU1065 (pSM007) Δ*yvrI*	(2)
HB7722	CU1065 (pSM009) Δ*yvrI-yvrHa*	(2)
HB7726	HB7709 (pSM009) Δ*yvrI-yvrHa*	(2)
HB7734	HB7726 (pSM004) *thrC*::P$_{oxdC}$-*lacZ*	(2)
HB7753	HB7722 (::*rpoC*-His$_6$) (Sp^r)	(2)
HB7754	HB7753 (pSM004) *thrC*::P$_{oxdC}$-*lacZ*	(2)
HB7756	HB7754 (pSM002) *amyE*::P$_{xyl}$-*yvrI-FLAG*	(2)
HB7759	HB7756 (pSM019) *lacA*::P$_{xyl}$-*yvrHa-HA* WT	(2)
HB7787	HB7720 (pSM004) *thrC*::P$_{oxdC}$-*lacZ*	This work
HB7794	HB7787 (pSM002) *amyE*::P$_{xyl}$-*yvrI-FLAG*	This work
HB7795	HB7787 (pSM028) *amyE*::P$_{xyl}$-*yvrI-FLAG* (Q166A)	This work
HB7796	HB7787 (pSM029) *amyE*::P$_{xyl}$-*yvrI-FLAG* (S169A)	This work
HB7818	HB7734 (pSM023) *lacA*::P$_{xyl}$-*yvrHa-HA* R41A	This work
HB7819	HB7734 (pSM024) *lacA*::P$_{xyl}$-*yvrHa-HA* E42A	This work
HB7820	HB7734 (pSM025) *lacA*::P$_{xyl}$-*yvrHa-HA* D43A	This work
HB7821	HB7734 (pSM042) *lacA*::P$_{xyl}$-*yvrHa-HA* L44A	This work
HB7822	HB7734 (pSM043) *lacA*::P$_{xyl}$-*yvrHa-HA* E45A	This work
HB7823	HB7734 (pSM026) *lacA*::P$_{xyl}$-*yvrHa-HA* Q46A	This work
HB7824	HB7734 (pSM027) *lacA*::P$_{xyl}$-*yvrHa-HA* E47A	This work
HB7825	HB7734 (pSM044) *lacA*::P$_{xyl}$-*yvrHa-HA* K49A	This work
HB7826	HB7734 (pSM045) *lacA*::P$_{xyl}$-*yvrHa-HA* K51A	This work
HB7827	HB7734 (pSM046) *lacA*::P$_{xyl}$-*yvrHa-HA* E54A	This work
HB7828	HB7734 (pSM047) *lacA*::P$_{xyl}$-*yvrHa-HA* K55A	This work
HB7839	HB7756 (pSM025) *lacA*::P$_{xyl}$-*yvrHa-HA* D43A	This work
HB7865	HB7734 (pSM019) *lacA*::P$_{xyl}$-*yvrHa-HA* WT	This work
HB7866	HB7756 (pSM019) *lacA*::P$_{xyl}$-*yvrHa-HA* WT	This work
HB7955	HB7734 (pSM178) *lacA*::P$_{xyl}$-*yvrHa-HA* D43N	This work
HB7956	HB7734 (pSM179) *lacA*::P$_{xyl}$-*yvrHa-HA* D43R	This work
HB7957	HB7734 (pSM180) *lacA*::P$_{xyl}$-*yvrHa-HA* L44E	This work
HB7958	HB7734 (pSM181) *lacA*::P$_{xyl}$-*yvrHa-HA* Q46E	This work
Plasmid	Construction and attributes (parental plasmid)	Source
pDG1663	Promoterless *lacZ* reporter vector (*thrC* integration)	(3)
pSWEET	Xylose-inducible expression vector (*amyE* integration)	(4)
pAX01	Xylose-inducible expression vector (*lacA* integration)	(5)
pET16b	IPTG-inducible *E. coli* expression vector	Novagen
pMAD	Generates unmarked in-frame deletions	(6)
pSM002	(pSWEET) 0.6-kb *yvrI*-FLAG gene PCR product used for conditional YvrI-FLAG expression vector in *B. subtilis*	This work
pSM004	(pDG1663) 0.45-kbp *yvrI-oxdC* intergenic region PCR product generates P*oxdC-lacZ* transcriptional fusion	This work
pSM016	(pAX01) 1.5-kbp kanamycin resistance gene PCR product used to replace erythromycin gene in pAX01	This work
pSM019	(pSM016) 0.27-kbp *yvrHa*-HA gene PCR product used for conditional YvrHa-HA expression in *B. subtilis*	This work
pSM028	(pSM002) Site-directed mutation in *yvrI* (Q166A)	This work
pSM029	(pSM002) Site-directed mutation in *yvrI* (S169A)	This work
pSM106	(pDG1663) 0.18-kbp PCR product carrying only *oxdC* promoter), generates P*oxdC-lacZ* transcriptional fusion	This work
pSM011	YvrI in pET16b	(2)
pSM082	YvrI (codons 1–108, N-terminus) in pET16b	This work
pSM083	YvrI (codons 108–192, C-terminus) in pET16b	This work
pSM017	YvrHa in pET16b	(2)
pSM012	SigA in pET16b	(2)

Strains	Parental strain, relevant genotype	Source
pWE100	SigM in pET16b	(7)
Two-hybrid plasmids		
pAC λcI	(control in two-hybrid analysis only)	(8)
pAC λcI-β831–1,057	Base plasmid for generating *NotI*/*BamH*I recombinants	(9, 10)
pBR α	(control in two-hybrid analysis only)	(8)
pBR α-β831–1,057	Base plasmid for generating *NotI*/*BamH*I recombinants	(9, 10)
pBR α-σ^{70}D581G	*E. coli* σ^{70} mutant (control in two-hybrid analysis only)	(9, 10)
pSM131	pBR α-YvrHa	This work
pSM132	pBR α-YvrI	This work
pSM133	pBR α-YvrI (N-terminus) (codons 1–108)	This work
pSM134	pBR α-YvrI (C-terminus) (codons 108–193)	This work
pSM136	pAC λcI-YvrI	This work
pSM137	pAC λcI-YvrI (N-terminus) (codons 1–108)	This work
pSM138	pAC λcI-YvrI (C-terminus) (codons 108–193)	This work
pSM139	pBR α-YvrHa (D43A)	This work
pSM143	pAC λcI-β-flap (codons 817–896)	This work
pSM144	pAC λcI-β′(codons 1–303)	This work
pSM148	pAC λcI-β-flap (codons 817–896) (I864K)	This work
pSM149	pAC λcI-β-flap (codons 817–896) (F865K)	This work
pSM159	pAC λcI-β′(codons 1–303) (R264Q)	This work
pSM160	pBR α-YvrHa (R41A)	This work
pSM162	pBR α-YvrHa (L44A)	This work
pSM164	pBR α-YvrHa (Q46A)	This work
pSM167	pBR α-YvrHa (D43N)	This work
pSM169	pBR α-YvrHa (L44E)	This work
pSM170	pBR α-YvrHa (Q46E)	This work
pSM172	pAC λcI-β′(codons 1–303) (E284K)	This work
pSM173	pAC λcI-β′(codons 1–303) (A291D)	This work

1. Deaconescu AM, et al. (2006) Structural basis for bacterial transcription-coupled DNA repair. *Cell* 124:507–520.
2. MacLellan SR, Wecke T, Helmann JD (2008) A previously unidentified sigma factor and two accessory proteins regulate oxalate decarboxylase expression in Bacillus subtilis. *Mol Microbiol* 69:954–967.
3. Guerout-Fleury AM, Frandsen N, Stragier P (1996) Plasmids for ectopic integration in Bacillus subtilis. *Gene* 180:57–61.
4. Bhavsar AP, Zhao X, Brown ED (2001) Development and characterization of a xylose-dependent system for expression of cloned genes in Bacillus subtilis: Conditional complementation of a teichoic acid mutant. *Appl Environ Microbiol* 67:403–410.
5. Hartl B, Wehrl W, Wiegert T, Homuth G, Schumann W (2001) Development of a new integration site within the Bacillus subtilis chromosome and construction of compatible expression cassettes. *J Bacteriol* 183:2696–2699.
6. Arnaud M, Chastanet A, Debarbouille M (2004) New vector for efficient allelic replacement in naturally nontransformable, low-GC-content, gram-positive bacteria. *Appl Environ Microbiol* 70:6887–6891.
7. Eiamphungporn W, Helmann JD (2008) The Bacillus subtilis sigma(M) regulon and its contribution to cell envelope stress responses. *Mol Microbiol* 67:830–848.
8. Dove SL, Hochschild A (2004) A bacterial two-hybrid system based on transcription activation. *Methods Mol Biol* 261:231–246.
9. Nickels BE, Dove SL, Murakami KS, Darst SA, Hochschild A (2002) Protein-protein and protein-DNA interactions of sigma70 region 4 involved in transcription activation by lambdacI. *J Mol Biol* 324:17–34.
10. Nickels BE, et al. (2005) The interaction between sigma70 and the beta-flap of Escherichia coli RNA polymerase inhibits extension of nascent RNA during early elongation. *Proc Natl Acad Sci USA* 102:4488–4493.